Supplementary Information

Crystal structure and luminescent properties of halocuprates with trimethylsulfonium cations

Andrey A. Petrov[a,b,‡,*], Luyi Chen[a,‡] , Mingming Li[a,*], Sergey A. Fateev[a,b], Andrey V. Petrov[c], Victor N. Khrustalev[d,e], Alexey B. Tarasov[b,f]

[a] Faculty of Materials Science, Shenzhen MSU-BIT University, 518172 Shenzhen, China

[b] Laboratory of New Materials for Solar Energetics, Department of Materials Science, Lomonosov Moscow State University, 119991 Moscow, Russia

[c] Institute of Chemistry, Saint Petersburg State University, 199034 Saint Petersburg, Russia

[d] Inorganic Chemistry Department, Peoples' Friendship University of Russia (RUDN University), 117198 Moscow, Russian Federation

[e] Zelinsky Institute of Organic Chemistry, Russian Academy of Sciences, 119991 Moscow Russia

[f] Department of Chemistry, Lomonosov Moscow State University, 119991 Moscow, Russian Federation

[‡] The first two authors contributed equally to this work.

* Corresponding authors: Andrey A. Petrov (basolon@gmail.com), Mingming Li (lmmhfut@163.com)

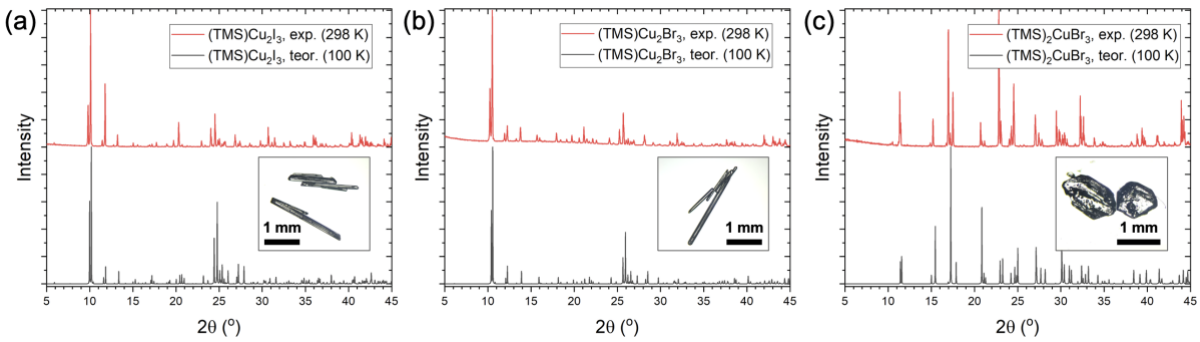

Fig. S1. Powder X-ray diffraction patterns from grinded crystals at 298 K (red), calculated diffraction patterns from crystal structures of single crystals refined at 100 K; insets: corresponding single ħcrystals of $(TMS)Cu_2I_3$, $(TMS)Cu_2Br_3$, and $(TMS)_2CuBr_3$.

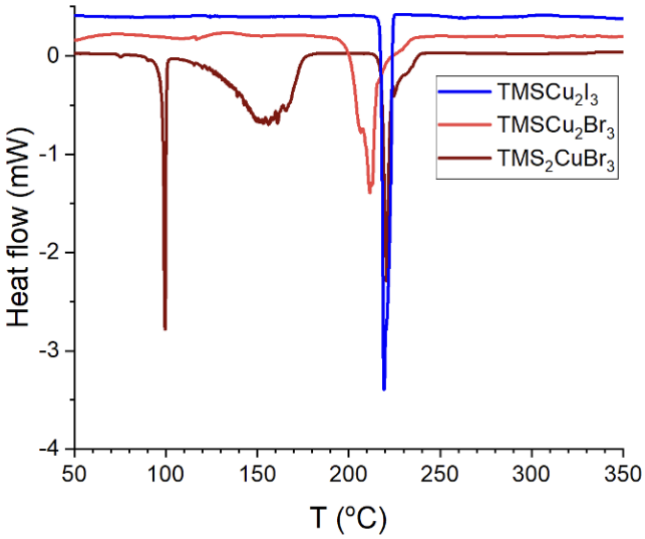

Fig. S2. DSC for $(TMS)Cu_2I_3$, $(TMS)Cu_2Br_3$, and $(TMS)_2CuBr_3$

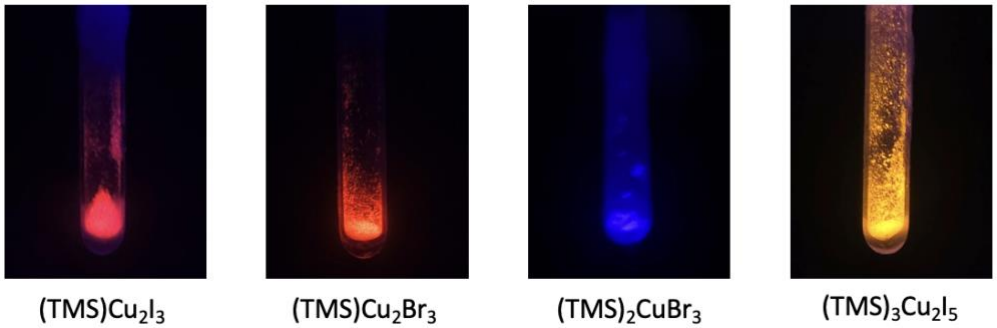

Fig. S3. Photoluminescence of trimethylsulfonium halocuprates at 77K at 254 nm.

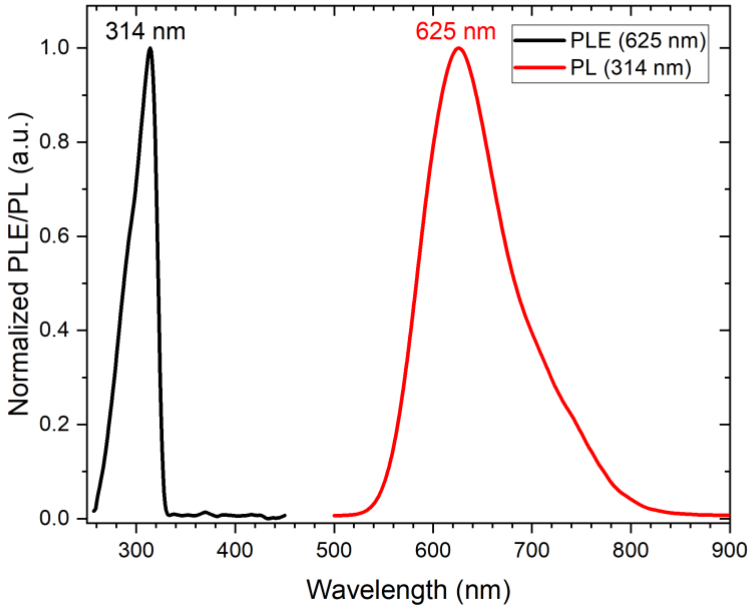

Fig. S4. PLE & PL spectra of (TMS)Cu_2Br_3 at 77K.

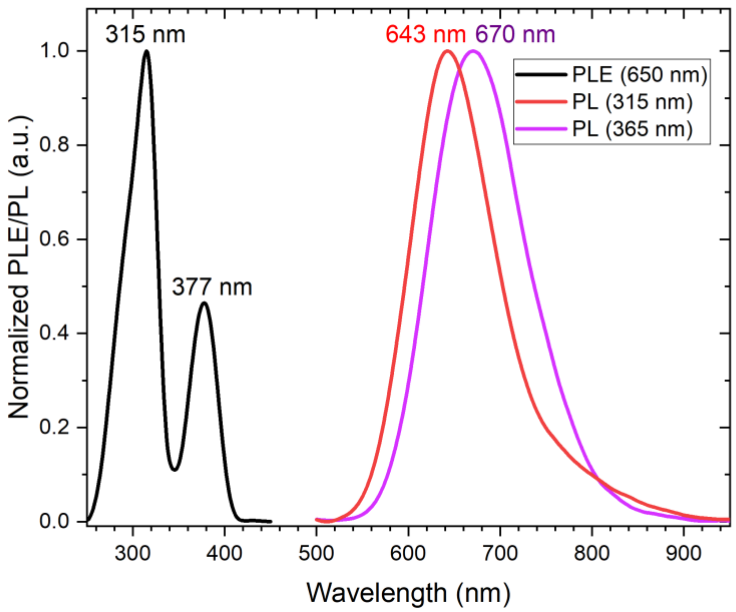

Fig. S5. PLE & PL spectra of (TMS)Cu_2I_3 at 77K.

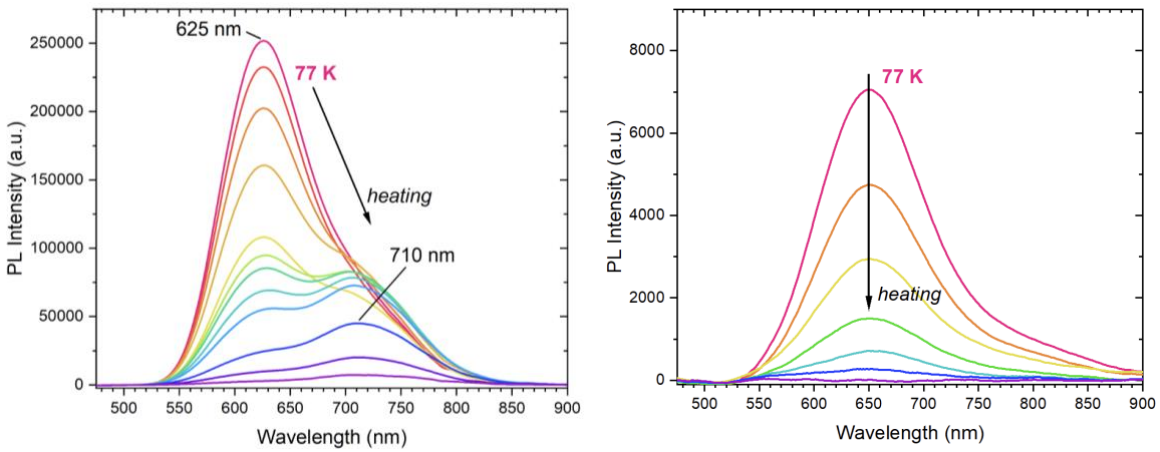

Fig. S6. Temperature-dependence of PL for $(TMS)Cu_2Br_3$ (a) and $(TMS)Cu_2I_3$ (b) at λ_{ex} = 254 nm.

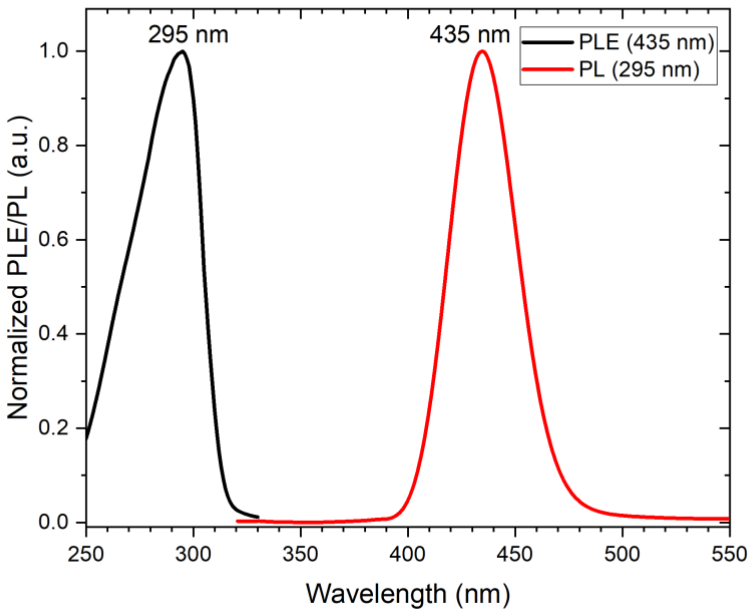

Fig. S7. PLE & PL spectra of $(TMS)_2CuBr_3$ at 77K.

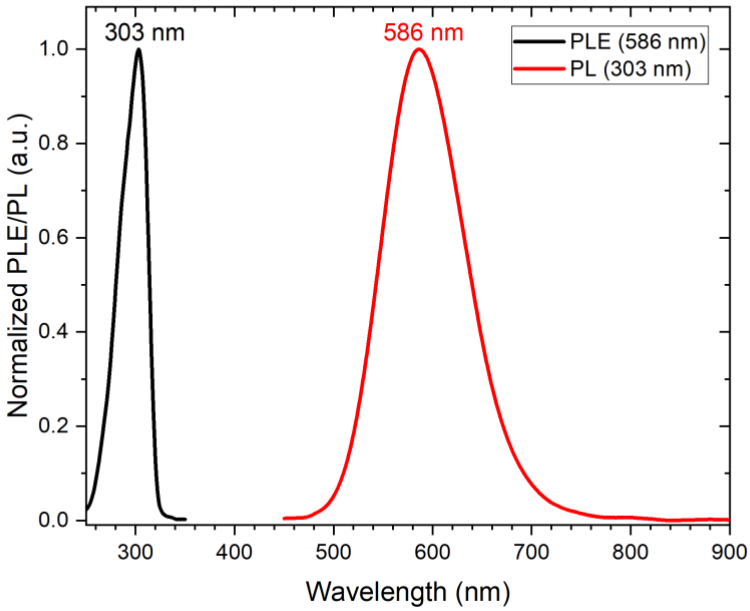

Fig. S8. PLE & PL spectra of $(TMS)_3Cu_2I_5$ at 77K.

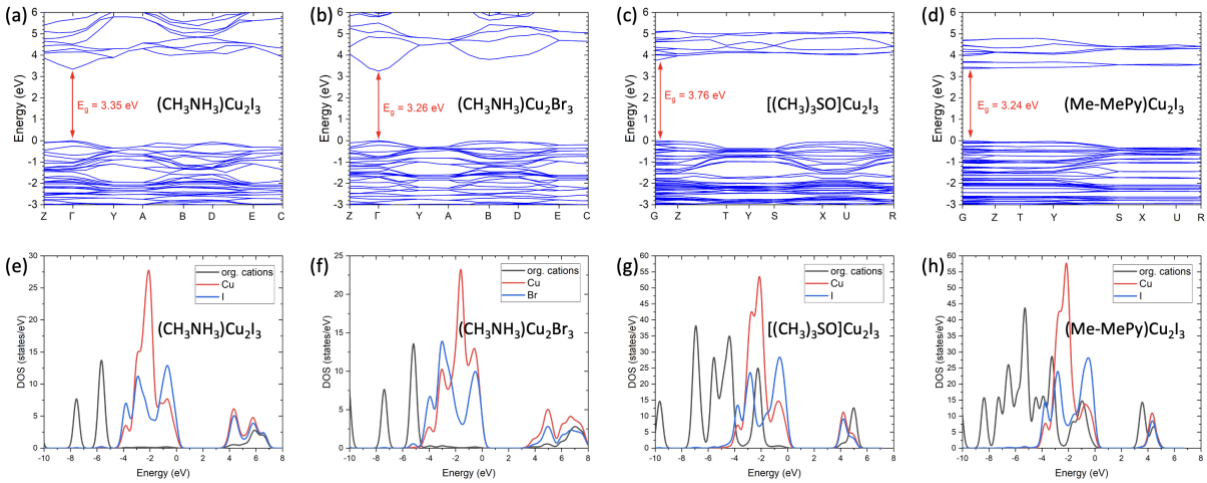

Fig. S7. Electronic structure of $(CH_3NH_3)Cu_2I_3$, $(CH_3NH_3)Cu_2Br_3$, $[(CH_3)_3SO]Cu_2I_3$, and $(Me\text{-}MePy)Cu_2I_3$).

Table S1. Parameters of the crystal structure refinement.

Phase	$TMSCu_2I_3$	$TMSCu_2Br_3$	TMS_2CuBr_3
Empirical formula	$C_9H_{24}I_9Cu_6S_3$	$C_3H_9Br_3Cu_2S$	$C_6H_{18}Br_3CuS_2$
M, g/mol	583.93	443.96	457.59
Crystal system	Orthorhombic	Orthorhombic	Monoclinic
Space group	*Pnma*	*Pnma*	*C2/c*
a, Å	17.7139(14)	17.0099(2)	14.3468(9)
b, Å	6.3941(6)	6.00199(8)	10.2589(6)
c, Å	29.860(2)	28.8341(3)	12.0601(8)
α, deg.	90.000	90.000	90.000
β, deg.	90.000	90.000	124.698(2)
γ, deg.	90.000	90.000	90.000
V, $Å^3$	3382.1(5)	2943.77(6)	1459.37(16)
Temperature (K)	100.0(2)	100.0(2)	100.0(2)
Z	12	12	12
D (calc), g/cm^3	3.440	3.005	2.083
μ, mm^{-1}	12.107	21.028	9.956
F(000)	3108	2472	880
Crystal size, mm	0.26 × 0.25 × 0.19	0.27×0.04×0.03	0.25×0.18×0.16
Θ range for data collection, deg.	3.568 – 56.862	3.048 – 79.615	2.63 – 30.48
Index ranges	$-23 \le h \le 23$ $-8 \le k \le 8$ $-39 \le l \le 39$	$-18 \le h \le 21$ $-6 \le k \le 7$ $-35 \le l \le 36$	$-19 \le h \le 20$ $-14 \le k \le 14$ $-17 \le l \le 12$
Reflections collected/independent	107527 / 4624	18385 / 3494	12727 / 2236
R_{int}	0.1174	0.0541	0.0747
Reflections with I>2σ(I)	4624	3291	1841
Goodness-of-fit on F	1.072	1.050	1.063
Final R indices ([I>2σ(I)])	$R_1 = 0.0336$ $wR_2 = 0.0740$	$R_1 = 0.0595$ $wR_2 = 0.1329$	$R_1 = 0.0304$ $wR_2 = 0.0634$
R indices (all data)	$R_1 = 0.0445$ $wR_2 = 0.0792$	$R_1 = 0.0620$ $wR_2 = 0.1341$	$R_1 = 0.0440$ $wR_2 = 0.0689$
Largest diff. peak/hole, $e/Å^3$	1.97 / -1.89	1.587 / -1.540	0.745 / -0.713

Table S2. Optical properties of the studied phases in comparison with other known halocuprates

	E_g, eV	**PL, eV**	**PLE, eV**	**Stokes shift, eV**	**PLQY, %**	**Ref**
RbCu_2Br_3	3.61	3.18 eV (RT)	4.59, 4.28	1.41, 1.10		[1]
CsCu_2I_3	3.63	2.17 (RT) 2.12 (77K)	3.71	1.56	3.23	[2]
CsCu_2Br_3	3.73	2.33 (RT) 2.32 (77K)	3.89	1.56	18.3	[2]
CsCu_2Cl_3	3.79	2.36 (RT) 2.32 (77K)	3.89	1.53	48	[2]
MACu_2I_3	3.62	2.06 (100K)				[3]
MACu_2Br_3	3.63	1.89 (77K)	3.63	1.74		[4]
TMSCu_2I_3	3.53	1.93 (77K), 1.85 (77K)*	3.94, 3.29	2.00, 1.44		This work
TMSCu_2Br_3	3.65	1.98 (77K) 1.75 (>77K)**	3.95	1.97		This work
NMPyCu_2I_3	2.85	1.84 1.77 (80K)	330	1.92	3.95	[5]
TMSOCu_2I_3	3.63	2.12 (RT)		1.49	<1%	[6]
DMACu_2Cl_3	3.80	2.05 (77K)				[7]

*when excited by light near the second PLE maximum, **at 77K < T < RT

Table S3. Cu-X bond distances in (TMS)Cu_2I_3, (TMS)Cu_2Br_3, and $(TMS)_2CuBr_3$.

Compound	Min. Distance (Å)	Max. Distance (Å)	Mean Distance (Å)	Std. Dev. (Å)
(TMS)Cu_2I_3	2.576	2.855	2.662	0.083
(TMS)Cu_2Br_3	2.415	2.591	2.496	0.069
$(TMS)_2CuBr_3$	2.362	2.398	2.374	0.018

Table S4. Parameters of the bond lengths and main distances in all studied structures.

Phase	Distortion index (bond length) [8]	Bond angle variance, deg. [8]	Cu···Cu distances, Å	Reference
$CsCu_2Br_3$	0.02890	12.6846	2.90660	[9]
$MACu_2Br_3$	0.02251	27.1412	2.754 2.816	[4]
$CsCu_2I_3$	0.01883	7.0799	3.14327	[9]
$MACu_2I_3$	0.01136	17.3062	2.883(9)	[3]
$(TMS)Cu_2Br_3$	(1) 0.02755; (2_1) 0.03091, 0.02590; (2_2) 0.03091, 0.2177	(1) 24.81; (2_1) 30.66, 25.07; (2_2) 30.66, 107.9;	2.902, 2.939	This work
$(TMS)Cu_2I_3$	(1) 0.01506; (2_1) 0.02888, 0.03042, 0.01326, 0.01151; (2_2) 0.02888, 0.02826, 0.01141, 0.01151;	(1) 21.98; (2_1) 41.26, 57.45, 23.12, 17.09; (2_2) 41.26, 101.80, 23.12, 90.47;	2.854, 2.870	This work

* symbols (1) and (2_x) stands for type-1 and type-2 Cu_2I_3 chains, subscript symbols q and 2 in (2_x) indicated the two different variants of type-2 chains according to specific choice of different partially occupied positions.

References:

[1] Ding Y, Lin R, Lin Z, Zheng W. Switchable biexcitons in perovskite-like $RbCu_2Br_3$ crystals driven by thermally induced phase transition. J Mater Chem C 2023;11:2531–9. https://doi.org/10.1039/D2TC05063C.

[2] Roccanova R, Yangui A, Seo G, Creason TD, Wu Y, Kim DY, et al. Bright Luminescence from Nontoxic $CsCu_2X_3$ (X = Cl, Br, I). ACS Mater Lett 2019;1:459–65. https://doi.org/10.1021/acsmaterialslett.9b00274.

[3] Petrov AA, Fateev SA, Grishko AY, Ordinartsev AA, Petrov AV, Seregin AY, et al. Optical properties and electronic structure of methylammonium iodocuprate as an X-ray scintillator. Mendeleev Commun 2021;31:14–6. https://doi.org/10.1016/j.mencom.2021.01.003.

[4] Belikova DE, Fateev SA, Khrustalev VN, Marchenko EI, Goodilin EA, Wang S, et al. Exceptional structural diversity of hybrid halocuprates(I) with methylammonium and formamidinium cations. Dalt Trans 2023;52:7152–60. https://doi.org/10.1039/D3DT00687E.

[5] Yue C-Y, Lin N, Gao L, Jin Y-X, Liu Z-Y, Cao Y-Y, et al. Organic cation directed one-dimensional cuprous halide compounds: syntheses, crystal structures and photoluminescence properties. Dalt Trans 2019;48:10151–9. https://doi.org/10.1039/C9DT01460H.

[6] Pinky T, Popy DA, Zhang Z, Jiang J, Pachter R, Saparov B. Synthesis and Characterization of New Hybrid Organic–Inorganic Metal Halides $[(CH_3)_3SO]M_2I_3$ (M = Cu and Ag). Inorg Chem 2024;63:2174–84. https://doi.org/10.1021/acs.inorgchem.3c04119.

[7] Belikova DE, Fateev SA, Khrustalev VN, Kozhevnikova V, Ordinartsev AA, Dzuban A V., et al. Bright luminescence of new low-melting copper(I) chlorides with compact organic cations. J Mater Chem C 2024;12:13537–44. https://doi.org/10.1039/D4TC02152E.

[8] Hazen RM, Downs RT, Prewitt CT. Principles of Comparative Crystal Chemistry. Rev Mineral Geochemistry 2000;41:1–33. https://doi.org/10.2138/rmg.2000.41.1.

[9] Hull S, Berastegui P. Crystal structures and ionic conductivities of ternary derivatives of the silver and copper monohalides—II: ordered phases within the $(AgX)_x$–$(MX)_{1-x}$ and $(CuX)_x$–$(MX)_{1-x}$ (M=K, Rb and Cs; X=Cl, Br and I) systems. J Solid State Chem 2004;177:3156–73. https://doi.org/10.1016/j.jssc.2004.05.004.